01 Jan 1983

Line-Adaptive Hybrid Coding of Images

Tai On Tam

John A. Stuller
Missouri University of Science and Technology, stuller@mst.edu

Recommended Citation

T. O. Tam and J. A. Stuller, "Line-Adaptive Hybrid Coding of Images," *IEEE Transactions on Communications*, vol. 31, no. 3, pp. 445 - 450, Institute of Electrical and Electronics Engineers, Jan 1983. The definitive version is available at https://doi.org/10.1109/TCOM.1983.1095824

Line-Adaptive Hybrid Coding of Images

TAI ON TAM, MEMBER, IEEE, AND JOHN A. STULLER, SENIOR MEMBER, IEEE

Abstract—**This paper describes novel adaptation strategy for hybrid transform/DPCM image coders. This strategy has yielded a 2–8 dB increase in signal-to-noise ratio in the transmission of a head and shoulders image at bit rates of 1–4 bits per pel and one-dimensional transform block sizes of 2–16.**

I. INTRODUCTION

This paper describes a novel hybrid transform/DPCM adaptation strategy [1] that has yielded a 2–8 dB increase in signal-to-noise ratio in the transmission of a head and shoulders image at bit rates of 1–4 bits/pel and one-dimensional transform block sizes of 2–16. Adaptive versions of Habibi's original hybrid transform/DPCM image coder [2] have previously been described by Roese [3], Jain [4], Jain and Wang [5], and Habibi [6]. A description of these coders and of the line-adaptive hybrid coder introduced here will be facilitated by reference to Fig. 1, which illustrates a typical nonadaptive hybrid coder. In this illustration, one-dimensional unitary transforms are taken along segments of an image line, followed by DPCM encoding of the resulting transform coefficients in the column direction. The decoded transform coefficients are inverse transformed at the receiver to produce the reconstructed picture elements (pels) of each line segment. Each of the M subarrays of Fig. 1 is coded independently of the others. The particular image frame segmentation of Fig. 1(a) is typical but not universal. For example, two-dimensional transforms can be taken within two-dimensional subblocks of an image followed by DPCM encoding of the transform coefficients among the subblocks [2].

Roese's adaptive coder [3] computes sample statistics of each column sequence of coefficient prediction error (Fig. 1) prior to coding and transmits these statistics to the receiver. These statistics are employed for adapting parameters and bit allocation for subsequent DPCM encoding of each coefficient column sequence. The bit assignments and predictor parameters are, in general, different for different subarrays. However, the total number of bits available for coding within each subarray is constrained to be equal. Roese's strategy is an example of *fixed-rate feedforward* adaptation, in which the adaptation parameters are fed forward to the receiver before coding takes place. Feedforward adaptation requires a preprocessing delay during which the adaptation parameters are computed from the input image, and "overhead" transmission bits to specify these parameters to the receiver. Since the image sample statistics and resulting adaptation parameters are derived from the input image prior to coding, these quantities are not contaminated by coding noise. Roese reports a 2.4–3.7 dB improvement in signal-to-noise ratio resulting from his adaptation strategy, using a source image similar to the one used in our study at bit rates of 0.5–2 bits/pel.

Jain [4] and Jain and Wang [5] have used another feedforward adaptation scheme in which each uncoded pel vector (Fig. 1) is classified into one of four activity classes, depending upon the sample variance of the pel vector. In this codec, the bit allocations in the DPCM loops are adapted to the image activity in each pel vector. This results in a *variable-rate feedforward* hybrid coder. Jain and Wang found that this adaptation procedure resulted in 5.5–8 dB improvement in signal-to-noise ratio in the transmission of a head and shoulders image at bit rates of 1–2 bits/pel. However, they judged the procedure to be somewhat impractical for on-line transmission because it requires identification of a large number of parameters for each image [5, p. 60].

Jain [4] and Jain and Wang [5] have also studied a *fixed-rate feedback* adaptation strategy in which sample statistics of each sequence of coefficient prediction error are estimated during coding. Here the quantizer adaptation is achieved by using only previously encoded DPCM data. Feedback adaptation does not required either a preprocessing delay or the transmission of overhead bits. It attempts to *predict* and adapt to the statistical parameters of data about to be coded, based upon previously coded data. Feedback adaptation assumes local stationarity of the image data and yields poor estimates of image statistics when local stationarity is not present. It can also yield poor estimates of image statistics for DPCM channels using a small number of bits since the estimates are derived from previously coded data, which is contaminated by the coding noise.

Habibi [6] also employs feedback adaptation to improve the performance of a hybrid coder. His codec uses a single quantizer and a variable-rate algorithm for coding the quantized coefficients. He reports a 3–4 dB improvement in signal-to-noise ratio in the encoding of an aerial view of a refinery.

II. LINE ADAPTIVE QUANTIZATION

The line adaptive hybrid coder employs fixed-rate feedforward adaptation of the DPCM quantizers. This adaptation is achieved on an image-line-to-image-line basis, requiring an encoding delay of one image line. This adaptive strategy permits the DPCM quantizers to be optimally adapted *both* to the image line that is about to be encoded *and* to the noisy coefficient predictions derived from previously coded lines.

As in Fig. 1, each N pel image line is partitioned into $M = N/I$ segments. A common quantizer Q_i is used in the DPCM encoding of the ith transform coefficients, $c_i(1)$, $c_i(2)$, $\cdots$, $c_i(M)$, obtained from the M line-segment transforms. Before the ith coefficient prediction errors $e_i(m) = c_i(m) - \hat{c}_i(m)$, $m = 1, 2, \cdots, M$, are quantized, the line-adaptive coder computes the sample variance σ_i^2 of the sequence $\{e_i(1), e_i(2), \cdots, e_i(M)\}$ of DPCM coder prediction errors. This sample variance is defined by

$$\sigma_i^2 = \frac{1}{M} \sum_{m=1}^{M} (e_i(m) - \eta_i)^2, \qquad 1 \leqslant i \leqslant I \tag{1a}$$

Paper approved by the Editor for Signal Processing and Communication Electronics of the IEEE Communications Society for publication without oral presentation. Manuscript received February 9, 1982; revised May 24, 1982. This work is based upon a thesis by T. O. Tam submitted in partial fulfillment of the M.S. degree from the University of Missouri at Rolla.

The authors are with the Department of Electrical Engineering, University of Missouri–Rolla, Rolla, MO 65401.

0090-6778/83/0300-0445$01.00 © 1983 IEEE

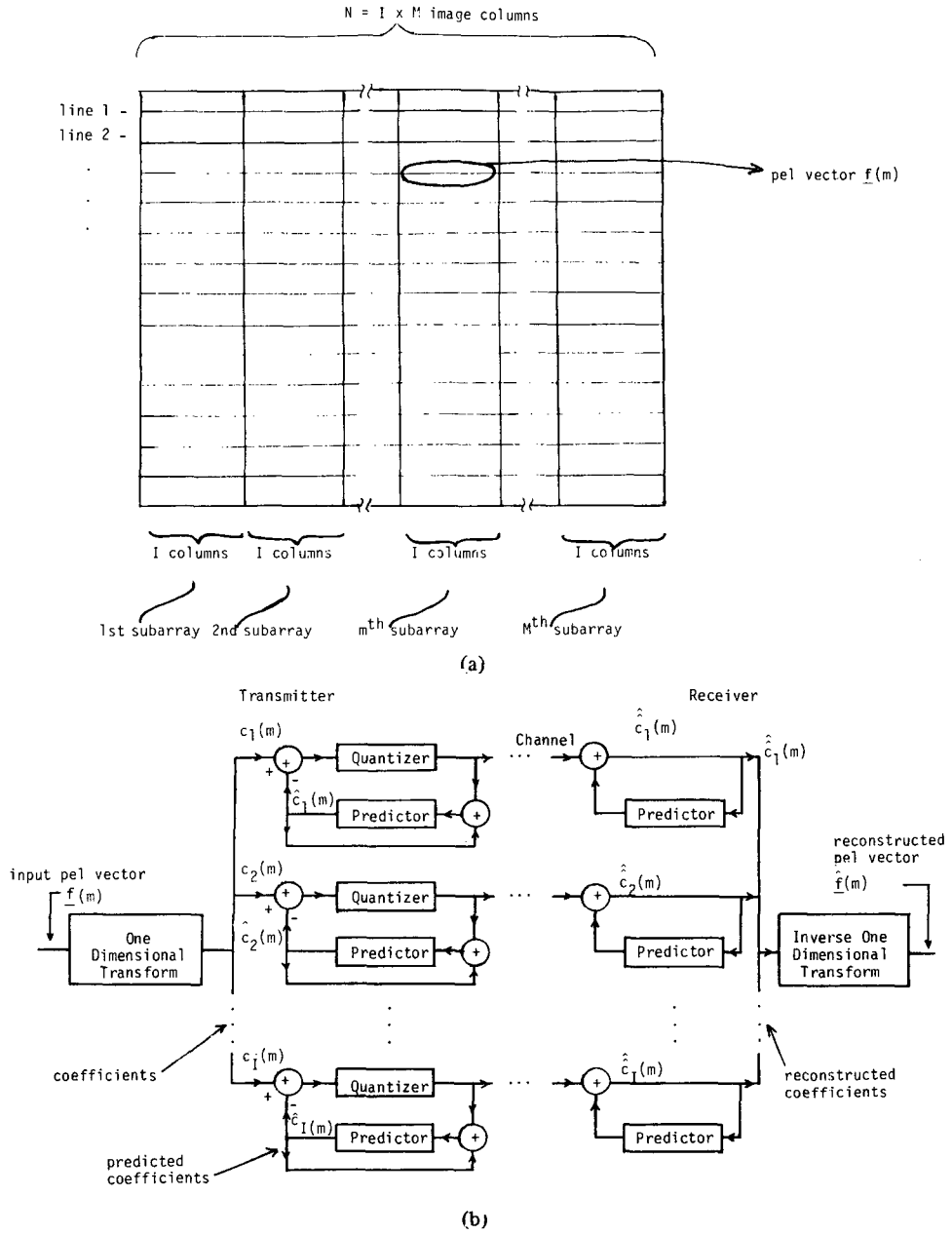

Fig. 1. Intraframe 1-D hybrid transform/DPCM codec. (a) Each horizontal line of the source image is partitioned into M segments of I pels each. (b) The vector of I pels of the mth segment is transformed, and each transform coefficient is predictively encoded columnwise. The receiver performs the inverse operations to produce the reconstructed image. The process is repeated for $m = 1, 2, \cdots, M$ and down subsequent lines.

where $e_i(m) = c_i(m) - \hat{c}_i(m)$ is the prediction error for coefficient c_i in the mth segment of the line, and η_i is the sample mean

$$\eta_i = \frac{1}{M} \sum_{m=1}^{M} e_i(m), \qquad 1 \leqslant i \leqslant I. \tag{1b}$$

The coder then quantizes σ_i^2 to obtain a b_i bit representation σ_i^{*2}, which is used to adapt Q_i for quantization of the prediction errors $e_i(1), e_i(2), \cdots, e_i(M)$. The b_i bit value of σ_i^{*2} is also transmitted to the receiver.

The method by which quantizer Q_i is adapted is shown in Fig. 2 in which a fixed quantizer Q_i^0 is optimized in the minimum mean square error sense [7] for a unit variance Laplacian input sequence [2]. Adaptation is achieved by dividing the coefficient prediction errors $e_i(m)$, $1 \leqslant m \leqslant M$, by σ_i^*. This normalizes the sample variance of the input to Q_i^0 to within a precision determined by b_i. Optimum quantization is then performed by Q_i^0 and the output levels are multiplied by σ_i^*.

Fig. 3 illustrates the adaptive codec subsystem used to encode the ith transform coefficients $c_i(1), c_i(2), \cdots, c_i(M)$. The "coefficient predictor memory" contains the entire sequence $\{\hat{c}_i(1), \hat{c}_i(2), \cdots, \hat{c}_i(M)\}$ of ith coefficient predictions for the present image line. The "prediction error memory"

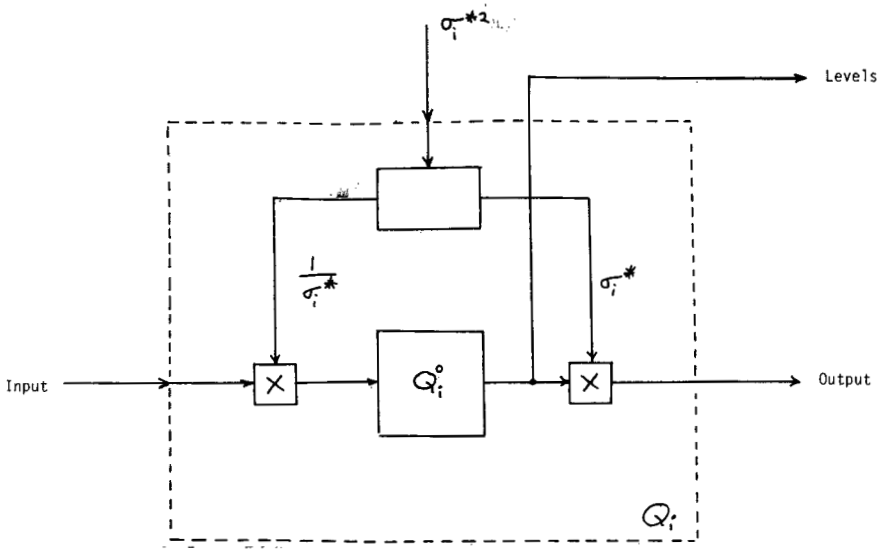

Fig. 2. Adaptive quantizer Q_i. The internal quantizer Q_i^0 is fixed and optimum in the minimum mean square error sense for a unit variance Laplacian input.

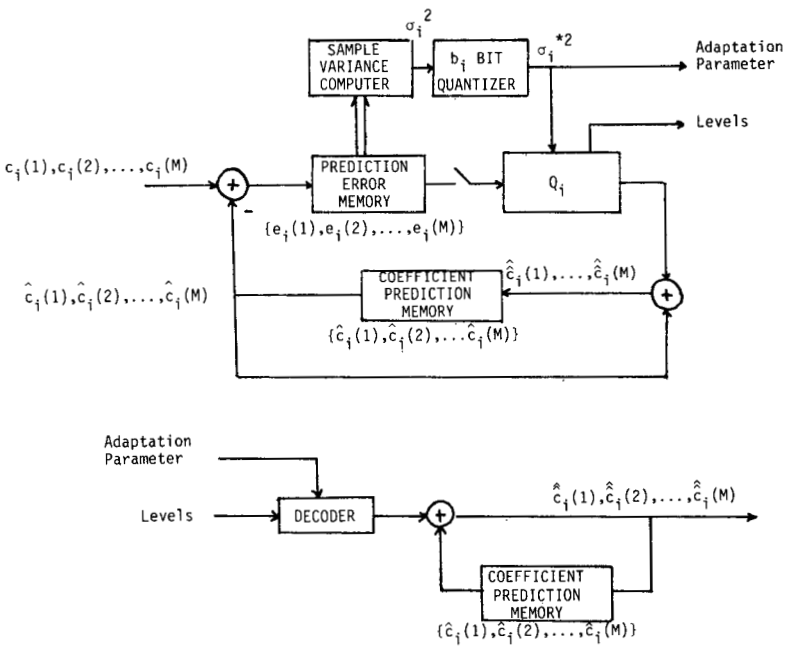

Fig. 3. Line-adaptive hybrid coder subsystem. The ith coefficient coder of Fig. 1 is modified to include 1) an M-stage coefficient memory and 2) an M-stage prediction error memory. Before coefficient encoding, the sample variance σ_i^2 of the ith coefficient errors is computed and is represented as a b_i bit quantity. This b_i bit representation of σ_i^2 is used to adapt quantizer Q_i.

contains the entire sequence $\{e_i(1), e_i(2), \cdots, e_i(M)\}$ of ith coefficient errors for the present image line. The contents of the coefficient predictor memory are read during the loading of the prediction error memory. The contents of the prediction error memory are then read (in entirety) to compute the sample variance σ_i^2 of (1) before quantization of the $e_i(m)$, $1 \leqslant m \leqslant M$. The quantized version of σ_i^2, σ_i^{*2}, adapts quantizer Q_i, which remains fixed during subsequent serial quantization of $e_i(1)$, $e_i(2)$, $\cdots$, $e_i(m)$. The quantized prediction errors add as quantized corrections to the predicted coefficient values at both the encoder and decoder to produce the decoded or reconstructed coefficients $\hat{\hat{c}}_i(1)$, $\hat{\hat{c}}_i(2)$, $\cdots$, $\hat{\hat{c}}_i(M)$.

Subsystems similar to that of Fig. 3 encode and decode coefficient sequences $\{c_i(1), c_i(2), \cdots, c_i(M)\}$, $i = 1, 2, \cdots, I$. The I decoded coefficients belonging to each mth line segment $\hat{\hat{c}}_1(m)$, $\hat{\hat{c}}_2(m)$, $\cdots$, $\hat{\hat{c}}_I(m)$ are then inverse transformed as in Fig. 1 to produce the reconstructed pel vector $\hat{f}(m)$ for that line segment. The decoded coefficient $\hat{\hat{c}}_i(m)$ is used directly as the predicted value of the corresponding coefficient of the upcoming line. This adaptive procedure is repeated on subsequent lines of the image, lending it the name line adaptive quantization (LAQ).

An important advantage of LAQ is that the quantizer Q_i is adapted to the particular error sequence $\{e_i(1), e_i(2), \cdots, e_i(M)\}$

that is to be input to the quantizer. This error sequence, with $e_i(m) = c_i(m) - \hat{c}_i(m)$, contains the DPCM coding error on $\hat{c}_i(m)$ arising from the coding of previous lines. Therefore, LAQ accounts for the previous line quantization error as well as the present line input in its quantizer adaptation. Minimization of prediction error quantization error by efficient adaptation of Q_i is important since in the DPCM system, coding error [here $c_i(m) - \hat{\hat{c}}_i(m)$] equals prediction error quantization error [4]. Again, since the hybrid coder employs a unitary transform, minimization of mean square error in the transform coefficient domain is equivalent to minimization of mean square error in the pel domain [8].

Instrumentation requires I subsystems having the structure of Fig. 3. This amounts to $N = I \times M$ words of memory for the coefficient predictions and N words of memory for the prediction errors. At low bit rates, the bit allocation may be such that not all I coefficients are encoded, and in this event fewer subsystems and less memory will be required. It should be noted that the computation of sample variance σ_i^2 can proceed during the quantization and transmission of the previous error sequence $\{e_{i-1}(1), e_{i-1}(2), \cdots, e_{i-1}(M)\}$. Therefore, the sample variance computer can be shared among the subsystems. It should also be noted that the sample variance σ_i^2 can be computed efficiently using the recursive formula [9]:

$$\sigma_i^2(m) = \sigma_i^2(m-1)(m-1)/m + [e_i(m) - \eta_i(m-1)]^2(m-1)/m^2 \quad (2a)$$

$$\eta_i(m) = \eta_i(m-1) + [e_i(m) - \eta_i(m-1)]/m \quad (2b)$$

where $\sigma_i^2(0) = \eta_i(0) = 0$. Further savings in equipment may be possible by sharing the prediction error quantizer Q_i [4] and the sample variance quantizer among the I subsystems.

Since b_i bits are used for transmitting the value of σ_i^2, the coder as described above will require

$$B_{OH} = \sum_{i=1}^{I} b_i$$

overhead bits per image line for its adaptation. It is possible to decrease this overhead by computing and transmitting the values of σ_i^2, $1 \leqslant i \leqslant I$, less frequently than once a line, keeping the quantizers fixed until the new variance information is transmitted. The bit rate of the adaptive coder can be determined as follows. Let r denote the rate of adaptation among image lines (such that $r = 1/k$ for adaptation every k lines). Let b_c denote the average number of quantizer bits assigned per coefficient, and let b_{oh} denote the average number of overhead bits per coefficient $b_{oh} = B_{OH}/I$. There are therefore Nb_c quantization bits and $rIb_{oh} = r(N/M)b_{oh}$ overhead bits transmitted per image line. The resulting total bit rate is therefore

$$R = b_c + rb_{oh}/M \text{ bits/pel.} \quad (3)$$

Equation (3) indicates that if b_c, b_{oh}, and r are fixed, the coder bit rate will decrease as the number M of subarrays is increased. For fixed line length N, increasing M also decreases the size of the $I = N/M$ point transform employed. This simplifies the implementation of the transform stage. However, increasing M also tends to reduce the effectiveness of the transform process because correlation among pels in *different* subarrays on each line is not exploited for redundancy reduction.

Fig. 4. Source image. The image array contains 256 × 256 8-bit picture elements.

III. SIMULATION

Nonadaptive and line-adaptive hybrid transform/DPCM image coders were simulated with Fortran software and the results were compared using the 256 by 256 8 bit/pel original of Fig. 4. Each coder employed the discrete cosine transform (DCT) [10], which is well known to be effective in transform and hybrid image coding [2], [8].

The quantizer characteristics of each coder were determined for minimum mean square error [2], [7], [11] based upon an assumed unit-variance Laplacian probability density function [2] for all the transform coefficient prediction errors. The prediction errors were scaled before quantization and the inverse of this scaling was applied to the quantizer outputs. The scale factors in the nonadaptive coder were fixed during the coding of each image, while those of the adaptive coder were varied among different image lines. Specifically, the prequantization scale factors of the nonadaptive coder were the reciprocals of the corresponding coefficient prediction-error standard deviations, computed without quantization for the image to be coded, with prediction error variances measured columnwise and averaged over all M segments. Consequently, the scale factors of the nonadaptive coder were individually matched to the global statistics of the input image. The scale factors used in the line-adaptive hybrid coder were the reciprocal standard deviations σ_i^{*-1}, with σ_i^2 computed linewise among the M line segments as in (2). Computation of σ_i^2 included previous-line quantization error as discussed in Section II and the result was represented as a b_i bit quantity. We observed in initial experiments that the maximum values of the σ_i^2 rarely exceeded 511. For simplicity we then chose $b_i = 9$ for each transmitted variance. More sophisticated methods for determining the b_i can certainly be devised, but based upon the numerical results of Section IV, we do not anticipate that their impact on total bit rate would be significant.

In the majority of the simulations, the bit allocations of each coder were identical. These bit allocations were determined by the methods of [2], [12]–[14] based upon the

TABLE I
BIT ALLOCATIONS OF HYBRID CODERS

	b_c	Coefficient Number															
	bits/pel	1	2	3	4	5	6	7	8	9	10	11	12	13	14	15	16
	4	5	3														
	3	4	2														
$I=2$	2	3	1														
	1.5	3	0														
	1	2	1														
	4	5	5	4	2												
	3	5	4	2	1												
$I=4$	2	4	3	1	0												
	1.5	3	2	1	0												
	1	3	1	0	0												
	4	5	5	5	5	4	3	3	2								
	3	5	4	4	3	3	2	2	1								
$I=8$	2	4	3	3	2	2	1	1	0								
	1.5	4	3	2	2	1	0	0	0								
	1	3	2	2	1	0	0	0	0								
	4	5	5	5	5	5	5	5	4	4	4	4	3	3	3	2	2
	3	5	5	5	4	4	4	4	3	3	3	2	2	2	1	1	0
$I=16$	2	5	4	4	3	3	3	2	2	2	1	1	1	1	0	0	0
	1.5	4	3	3	3	2	2	2	2	1	1	1	0	0	0	0	0
	1	4	3	2	2	2	1	1	1	0	0	0	0	0	0	0	0

global coefficient prediction error variances of the image to be coded and the coding bit rate desired. The bit allocation maps are given in Table I.

In each simulation, the normalized mean square error (NMSE) was computed for an objective measure of system performance. The NMSE is defined as

$$\text{NMSE} = \frac{\langle (f-\hat{f})^2 \rangle}{\langle f^2 \rangle} \ 100 \text{ percent}$$

in which f and $\hat{f}$ denote original and coded pel intensity values, respectively, and $\langle\langle \cdot \rangle\rangle$ denotes arithmetic average over all 256 X 256 pels. Corresponding to this NMSE is the signal-to-noise ratio (SNR) [4]

$$\text{SNR} = 10 \log_{10} \left\{ \frac{\langle f^2 \rangle}{\langle (f-\hat{f})^2 \rangle} \right\}.$$

IV. RESULTS

Table II lists SNR and NMSE performance results of nonadaptive and line-adaptive hybrid coding. These results were obtained by using the source image of Fig. 4 and line segment subarray sizes of $I = 2$, 4, 8, and 16. The left-hand column of these tables contains the average quantizer bit rates b_c of each coder. The right-hand column contains the additional bit rates necessary for specifying the variances σ_i^2 in line adaptive coding. The line adaptation rate was $r = 1/2$. In consequence of (3), the impact of adaptation on the total bit rate can be seen to increase with subarray size, $I = N/M$. This increase is 1 or 2 percent for $I = 2$, and 7–15 percent for $I = 16$. Quantizer bit allocations corresponding to Table II are given in Table I. It can be seen from Table II that for bit rates ranging from 1 to 4 bits/pel, line adaptation increases SNR by about 4–7 dB for subarray sizes $I = 2$, 4, and 8. The increase in SNR for $I = 16$ varied from about 2 dB at 4 bits/pel to nearly 8 dB at 1.5 bits/pel. It should be emphasized that the quantizers used in the nonadaptive hybrid coder were matched to the source image of Fig. 4. Therefore, the performance of nonadaptive hybrid coders whose quantizers are matched to a larger ensemble of source images should be below that of this nonadaptive coder for this particular source image.

(a)

(b)

Fig. 5. Results of coding. (a) Nonadaptive hybrid coder using one-dimensional block size $I = 8$ with coding rate 1 bit/pel. SNR = 20.42 dB. (b) Line-adaptive hybrid coder using one-dimensional block size $I = 8$ with coding rate 1.07 bits/pel. Line adaptation rate $r = 0.5$. SNR = 27.41 dB.

Fig. 5 shows representative coded images for both nonadaptive and line-adaptive coding using a one-dimensional block size $I = 8$ and quantization bit rate $b_c = 1$ bit/pel. The line-adaptive coder used a line adaptation rate $r = 0.5$, which required an additional 0.07 bit/pel for transmission. The visual improvment obtained with LAQ was particularly dramatic in this example and appears to occur primarily in the vicinity of luminance edges. In every experiment we performed, LAQ resulted in coded images that had greater fidelity than those of the nonadaptive hybrid coder. The nature of the improvement was qualitatively similar to that seen in Fig. 5.

Exploratory simulations were performed using other line adaptation rates. In these simulations a line adaptation rate $r = 1$ yielded only slight additional improvement (0.1–0.5 dB) in SNR at the expense of doubling the overhead bit rate. Performance degraded progressively as r was decreased.

Exploratory simulations were performed using source images of different types, such as aerial scenes. In all experiments, the improved performance of the line-adaptive hybrid coder was in basic agreement to that shown in Table II.

TABLE II
PERFORMANCE OF HYBRID CODERS

		Nonadaptive		Line Adaptive		Overhead
	b_c bits/pel	SNR (dB)	NMSE (%)	SNR (dB)	NMSE (%)	bits/pel
	4	34.03	0.0395	38.91	0.0129	0.035
	3	27.96	0.1601	34.23	0.0377	0.035
$I = 2$	2	22.33	0.5848	28.90	0.1287	0.035
	1.5	21.59	0.6943	25.93	0.2554	0.018
	1	16.97	0.2008	23.25	0.4728	0.018
	4	33.66	0.0431	38.28	0.0149	0.070
	3	31.61	0.0691	36.15	0.0243	0.070
$I = 4$	2	26.64	0.2170	31.92	0.0643	0.053
	1.5	21.64	0.6852	28.57	0.1392	0.053
	1	20.58	0.8741	25.23	0.2998	0.035
	4	31.85	0.0653	35.24	0.0299	0.141
	3	30.12	0.0972	35.03	0.0314	0.141
$I = 8$	2	25.20	0.3021	32.89	0.0514	0.123
	1.5	24.56	0.3502	30.94	0.0805	0.088
	1	20.42	0.9081	27.41	0.1817	0.070
	4	29.82	0.1041	31.98	0.0634	0.281
	3	29.75	0.1060	32.57	0.0553	0.264
$I = 16$	2	28.34	0.1464	32.82	0.0523	0.229
	1.5	23.57	0.4397	31.48	0.0712	0.193
	1	22.15	0.6100	28.37	0.1457	0.141

An exploratory simulation was also performed to determine the improvement resulting by adapting bit allocation among the I quantizers on a line-to-line basis, keeping the average number of quantizer bits per coefficient equal for each line. The bit allocation was determined from the quantized sample variances σ_i^{*2}, $i = 1, 2, \cdots, I$, by the methods of [2], [12]–[14]. This complex scheme yielded only 0.5 dB improvement in SNR for the source image of Fig. 4 with $r = 1$ and $I = 4$ compared to LAQ.

V. CONCLUSION

The experimental results indicate that the feedforward LAQ provides an effective means to increase the performance of the hybrid coding system. Even though this makes the hardware implementation somewhat more complex by requiring additional memory and separate transmission of variance information, the improvement may justify the use of LAQ in some applications.

ACKNOWLEDGMENT

The authors are grateful to the reviewers for several constructive suggestions. The authors also thank H. W. Paik for his assistance in photographing the images.

REFERENCES

[1] T. O. Tam, "Study of a hybrid transform/DPCM coder," M.S. thesis, Univ. Missouri, Rolla, 1981.
[2] A. Habibi, "Hybrid coding of pictorial data," *IEEE Trans. Commun.*, vol. COM-22, pp. 614–624, May 1974.
[3] J. A. Roese, "Hybrid transform/predictive image coding," in *Advances in Electronics and Electron Physics*, Suppl. 12. New York: Academic, 1979, pp. 157–187.
[4] A. K. Jain, "Image data compression: A review," *Proc. IEEE*, vol. 69, pp. 349–389, Mar. 1981.
[5] A. K. Jain and S. H. Wang, "Stochastic image models and hybrid coding," Dep. Elec. Eng., State Univ. New York, Buffalo, Final Rep., NOSC Contr. N00953-77-C-003MJE, Oct. 1977.
[6] A. Habibi, "An adaptive strategy for hybrid image coding," *IEEE Trans. Commun.*, vol. COM-29, pp. 1736–1740, Dec. 1981.
[7] J. Max, "Quantizing for minimum distortion," *IRE Trans. Inform. Theory*, vol. IT-6, pp. 7–12, Mar. 1960.
[8] W. K. Pratt, *Digital Image Processing*. New York: Wiley, 1978.
[9] M. Schwartz, *Signal Processing: Discrete Spectral Analysis, Detection and Estimation*. New York: McGraw-Hill, 1975, no. 3.9, p. 143.
[10] N. Ahmed, T. Natarajan, and K. R. Rao, "Discrete cosine transform," *IEEE Trans. Comput.*, vol. C-23, pp. 90–93, Jan. 1974.
[11] M. D. Paez and T. H. Glisson, "Minimum mean-square-error quantization in speech PCM and DPCM systems," *IEEE Trans. Commun.*, vol. COM-20, pp. 225–230, Apr. 1972.
[12] J. J. Y. Huang and P. M. Schultheiss, "Block quantization of correlated Gaussian random variables," *IRE Trans. Commun. Syst.*, vol. CS-11, pp. 289–296, Sept. 1963.
[13] A. Segall, "Bit allocation and encoding for vector sources," *IEEE Trans. Inform. Theory*, vol. IT-22, pp. 162–169, Mar. 1966.
[14] R. C. Wood, "On optimum quantization," *IEEE Trans. Inform. Theory*, vol. IT-15, pp. 248–252, Mar. 1969.

Diversity ALOHA—A Random Access Scheme for Satellite Communications

GAGAN L. CHOUDHURY AND STEPHEN S. RAPPAPORT, SENIOR MEMBER, IEEE

***Abstract*—A generalization of the slotted ALOHA random access scheme is considered in which a user transmits multiple copies of the same packet. The multiple copies can be either transmitted simultaneously on different frequency channels (frequency diversity) or they may be transmitted on a single high-speed channel but spaced apart by random time intervals (time diversity). In frequency diversity, two schemes employing channel selections with and without replacements**

Paper approved by the Editor for Space and Satellite Communication of the IEEE Communications Society for publication after presentation at GLOBECOM '82, Miami, FL, December 1982. Manuscript received December 28, 1981; revised June 24, 1982. This work was supported in part by the National Science Foundation under Grant ECS-80-25312.

The authors are with the Department of Electrical Engineering, State University of New York, Stony Brook, NY 11794.

0090-6778/83/0300-0450$01.00 © 1983 IEEE